Analysis of calorimetric measurements of grain growth

L. C. Chen[a] and F. Spaepen
Division of Applied Sciences, Harvard University, Cambridge, Massachusetts 02138

(Received 21 May 1990; accepted for publication 27 August 1990)

A method for extracting the parameters describing the process of grain growth from calorimetric data is presented. Both isothermal and scanning experiments are considered. It is demonstrated that the Kissinger method used for determining the activation enthalpy of a nucleation-and-growth process can be used for a grain growth process as well. Characteristic differences between the signals, both scanning and isothermal, from nucleation-and-growth and grain growth are pointed out. These are useful for distinguishing truly amorphous structures from microcrystalline ones by their transformation behavior. As an example, the method is applied to a study of grain growth in microquasicrystalline Al-Mn thin films.

I. INTRODUCTION

Differential calorimetry is a convenient and widely used method for studying the kinetics of phase transformations. This can be done in either the isothermal or linear heating (scanning) mode. In isothermal experiments the transformed fraction, proportional to the integrated signal, is determined as a function of time, and is usually fit to the Johnson-Mehl-Avrami (JMA) formalism[1] to determine the mechanisms that govern nucleation and growth. The JMA parameters can also be obtained from scanning experiments. The Kissinger[2] analysis of the shift of the transformation peaks as a function of heating rate is perhaps the best known method for this purpose. Henderson[3] has published a critical analysis of these nonisothermal methods which shows under what conditions the Kissinger method is rigorously justified.

Grain growth is usually studied by direct observation in the optical or electron microscope. The release of interfacial (grain boundary) enthalpy in this process is usually too small to be measurable in the calorimeter. If the grain size is less than about 10 nm, however, as in microcrystalline materials prepared by rapid solidification[4] or vapor deposition,[5] or in some of the materials prepared by gas condensation and compaction,[6] precise direct measurements become difficult. The large interface-to-volume ratio in these materials, on the other hand, makes it possible to monitor grain growth calorimetrically, at least if the grain boundary mobility is relatively high, as in metals.[7,8]

This paper shows how such calorimetric data can be analyzed to extract the parameters that characterize the grain growth process. In particular, it is shown that the Kissinger method can be applied to peaks resulting from grain growth. Furthermore, the characteristic differences between the calorimetric signals for nucleation-and-growth and grain growth can be used to determine whether a material with broad diffraction peaks is truly amorphous (liquidlike) or microcrystalline.[7] As an example, the analysis is applied to grain growth in microquasicrystalline sputtered Al-Mn films.

II. DESCRIPTION OF THE GRAIN GROWTH PROCESS

In normal grain growth, the larger grains in a population grow, on the average, at the expense of the smaller ones. The driving force for this process is the decrease in interfacial free energy. If the interfacial tension, γ, and the mobility, M, of the grain boundaries are assumed constant, the increase in the average radius, r, of the grains can be written as

$$\frac{dr}{dt} = \frac{cM\lambda^n\gamma}{r^{n-1}}, \tag{1}$$

where c is a numerical factor, λ is the interatomic distance, and n is an exponent, empirically between 1.5 and 4.[9] Theoretical grain growth models give $n = 2$.[10–13] Standard transition state rate theory[1] gives the mobility in terms of microscopic quantities as:

$$M = \nu\lambda^2/k_BT, \tag{2}$$

where ν is the net jump frequency across the boundary and k_B is Boltzmann's constant. The jump across the boundary is usually assumed to be a singly activated process, so that

$$\nu = \nu_0 \exp(-Q/k_BT). \tag{3}$$

Equation (1) can be integrated to give the evolution of the grain size as

$$r^n(t) = r^n(0) + \int_0^t k(T)dt, \tag{4}$$

where

$$k(T) = ncM\lambda^n\gamma. \tag{5}$$

For convenience, the temperature dependence of this rate constant can be rewritten as

$$k(T) = (k_0/T)\exp(-Q/k_BT). \tag{6}$$

This factor is sometimes also assumed to have a simple Arrhenius-type temperature dependence:

$$k(T) = k_0' \exp(-Q'/k_BT). \tag{7}$$

This assumption is based on an incorrect treatment of the frequency factor in the mobility,[14,15] but, as will be shown

[a] Present address: General Electric Research and Development Center, Schenectady, New York 12301.

 0021-8979/91/020679-10$03.00

later, over the relatively narrow temperature range of the transformations under consideration here, the difference between the activation enthalpies obtained from Eqs. (6) or (7) is negligible. Since in the original Kissinger analysis the rate constant is treated in the same way as in Eq. (7), the analysis below will be carried out for both equations.

In an isothermal experiment the evolution of the grain size is

$$r^n(t) = r^n(0) + k(T)t. \tag{8}$$

In a scanning experiment, at constant heating rate $b = dT/dt$, the grain size evolution is

$$r^n(t) = r^n(0) + \int_0^T \frac{k(T)}{b}\,dT = r^n(0) + I(T)/b. \tag{9}$$

The total interfacial enthalpy of a system with volume V and average grain radius r is

$$H = g\gamma_H V/r, \tag{10}$$

where γ_H is the enthalpic part of the interfaced tension, and g is a numerical factor, on the order of unity, that depends on the shape and size distribution of the grains. The evolution of the interfacial enthalpy can then be written as

$$H(t) = H_0 r_0/r(t), \tag{11}$$

where H_0 and r_0 are, respectively, the initial enthalpy and grain radius.

The calorimetric signal is the rate, $\dot{H}$, at which the enthalpy of the sample changes (a negative quantity for exothermal processes). Combining Eqs. (11), (8), (5), and (1) gives

$$\dot{H} = -\frac{H_0 r_0}{r^2}\frac{dr}{dt} = -\left(\frac{H_0 r_0}{n}\right)\frac{k(T)}{r^{n+1}}. \tag{12}$$

In an isothermal experiment:

$$-\dot{H} = \left(\frac{H_0 r_0}{n}\right)\frac{k(T)}{[r_0^n + k(T)t]^{(n+1)/n}}. \tag{13}$$

In a scanning experiment

$$-\dot{H} = \left(\frac{H_0 r_0}{n}\right)\frac{k(T)}{[r_0^n + I(T)/b]^{(n+1)/n}}. \tag{14}$$

III. DETERMINATION OF THE ACTIVATION ENTHALPY FROM SCANNING EXPERIMENTS—THE KISSINGER ANALYSIS

In the standard Kissinger analysis of a nucleation-and-growth process the activation enthalpy of the rate constant is determined by plotting, for a number of scans at different rates b, $\ln(b/T_p^2)$ vs $(1/T_p)$, where T_p is the peak temperature (maximum rate) of the transformation. The slope of a straight line fit through the plot is then Q/k_B. We show now that the same analysis applies to a grain growth process as well.

The condition for a peak in the enthalpy release rate is

$$\frac{\partial \dot{H}}{\partial T} = 0. \tag{15}$$

Differentiating Eq. (14) leads to the condition, at $T = T_p$:

$$\frac{\partial k(T_p)}{\partial T}\left(r_0^n + \frac{I(T_p)}{b}\right) = \frac{n+1}{n}\frac{[k(T_p)]^2}{b}. \tag{16}$$

If the temperature dependence of the rate constant is described by Eqs. (6) or (7), the respective integrals can be evaluated:

$$I(T) = k_0 E_1(Q/k_B T); \tag{17a}$$

$$I(T) = k_0' T E_2(Q'/k_B T), \tag{17b}$$

where $E_1(x)$ and $E_2(x)$ are exponential integral functions.[16] Since, as will be shown experimentally below, for the temperature range of interest here Q, $Q' \gg k_B T$, the large argument approximation of these functions can be used:

$$E_1(x) \approx E_2(x) \approx (x e^x)^{-1}. \tag{18}$$

The integrals of Eqs. (17) then both become:

$$I(T) = (k_B T^2/Q)k(T). \tag{19}$$

For both equations (6) and (7) one can write, again under the condition Q, $Q' \gg k_B T$:

$$\frac{\partial k(T)}{\partial T} = \frac{Q}{k_B T^2}k(T). \tag{20}$$

Inserting Eqs. (19) and (20) into the condition of Eq. (16) then gives in both cases:

$$\frac{Q r_0^n}{k_B T_p^2} = \frac{k(T_p)}{nb}. \tag{21}$$

For the rate constant of Eq. (6) this can be rewritten as

$$A\frac{b}{T_p} = \exp\left(-\frac{Q}{k_B T_p}\right), \tag{22}$$

where A is a temperature-independent constant. This equation shows that $-Q/k_B$ is the slope of a plot of $\ln/(bT_p)$ vs $1/(T_p)$.

For the rate constant of Eq. (7) the condition of Eq. (21) becomes

$$A'\frac{b}{T_p^2} = \exp\left(-\frac{Q'}{k_B T_p}\right), \tag{23}$$

where A' is again a temperature-independent constant. In this case $-Q'/k_B$ is the slope of a plot of $\ln/(bT_p^2)$ vs $(1/T_p)$. This is the same as in the traditional Kissinger analysis. In all cases $Q' < Q$. As will be shown below, however, for the usual conditions in calorimetric experiments, the values of Q and Q' are almost identical. This is confirmed by the analysis of numerically simulated DSC scan data, where the activation enthalpy is known *a priori*. For example, a set of scans generated by numerical integration of Eq. (14) with an assumed activation enthalpy of 2.04 eV gave $Q = 2.02$ eV and $Q' = 1.97$, when analyzed according to Eqs. (22) and (23), respectively.

IV. DETERMINATION OF THE GRAIN GROWTH EXPONENT

The grain growth exponent, n, can be obtained most accurately from an isothermal experiment. Using the definition

$$\tau = r_0^n/k(T), \tag{24}$$

the direct signal, i.e., the isothermal enthalpy release rate of Eq. (13), can be rewritten as

$$-\ln(-\dot{H}) = (1+1/n)\times\ln(t+\tau) + \ln\left(\frac{k^{1/n}n}{H_0 r_0}\right). \tag{25}$$

If τ is chosen so that a plot of $-\ln(-\dot{H})$ vs $\ln(t+\tau)$ is a straight line, its slope corresponds to $(1+1/n)$. The problem with this procedure is that it is not very precise. For example, if $n=2$, a 10% error in the slope corresponds to a 40% error on the value of the exponent.

A more precise method is to use the integrated signal, i.e., the total interfacial enthalpy:

$$H(t) = H_0 + \int_0^t \dot{H}\,dt. \tag{26}$$

Combining Eqs. (8) and (11) gives

$$H(t) = \frac{H_0 r_0}{r} = \frac{H_0 r_0}{[r_0^n + k(T)t]^{1/n}}, \tag{27}$$

or

$$\left(\frac{H(t)}{H_0}\right)^n = \frac{r_0^n}{r_0^n + k(T)t} = \frac{\tau}{t+\tau}. \tag{28}$$

A plot of $\ln(t+\tau)$ vs $\ln(H/H_0)$ therefore has a slope $-n$, and the fractional error of the exponent is the same as that of the slope. The latter is estimated at about 10%, corresponding to the range of values for τ for which the plot is judged to be a straight line.

V. DETERMINATION OF THE ACTIVATION ENTHALPY FROM ISOTHERMAL EXPERIMENTS

The activation enthalpy of the rate constant can also be determined by performing a series of isothermal experiments at different temperatures. Since a different amount of grain growth occurs during heatup to these different temperatures, the initial interfacial enthalpy $H_0(T)$ depends on the holding temperature. It is directly measurable by integrating the entire isothermal signal, since $H(t)$ in Eqs. (11) and (26) becomes negligibly small for r, $t\to\infty$. The time $t_{1/2}$ is defined as the time required to lower the stored interfacial enthalpy to half its initial value $H(t_{1/2},T) = H_0(T)/2$. Since the grain size doubles over that time, the following condition is obtained from Eq. (8):

$$(2^n - 1)r_0^n(T) = k(T)t_{1/2}. \tag{29}$$

Using Eq. (10) this can be rewritten as

$$H_0^n(T)k(T)t_{1/2} = C, \tag{30}$$

where C is a temperature-independent constant. Depending on the form of the temperature dependence of $k(T)$ [Eq. (6) or (7)], the slope of a straight-line fit of $\ln[t_{1/2}H_0^n(T)]$ or $\ln[t_{1/2}H_0^n(T)/T]$ vs $1/T$ corresponds to, respectively, Q'/k_B or Q/k_B.

It is generally useful to compare the results of the two methods for determining the activation enthalpies, since it provides a check on the assumptions of the formalism, such as the temperature- and size-independence of γ or k.

VI. DETERMINATION OF THE REMAINING PARAMETERS

The actual value of the grain size cannot be determined from calorimetric data only. In the analysis, it always occurs together with the kinetic parameter, k, as in the measurable parameter $\tau = r_0^n/k(T)$, defined in Eq. (24), for example. The value of r_0, or the value of r at any other time, must therefore be obtained from other observations. The most direct technique is high-resolution electron microscopy.[8] It is often difficult to observe the initial grain size directly, since even in the thinnest samples many nm-size grains overlap. Measurements of the grain size after some growth are somewhat more feasible. A second technique is based on the broadening of the diffraction peaks,[5,17] but this is somewhat model dependent. Although a precise determination of the absolute grain size is therefore difficult, it is possible to get a reasonable estimate if the two methods give similar results.

Once r_0 is known, the average enthalpic part of the interfacial tension, γ_H, can be estimated from the area under the transformation peak in a scanning experiment, i.e., H_0, and Eq. (10). The main uncertainty here is the value of the geometrical constant, g, which depends on the shapes and size distribution of the grains. As shown in Appendix A, for equiaxed grains g is estimated at 1.3 ± 0.2, which gives an uncertainty of about 30% for γ_H.

VII. COMPARISON OF THE CALORIMETRIC SIGNAL FROM TRANSFORMATIONS OCCURRING BY NUCLEATION-AND-GROWTH OR BY GRAIN GROWTH.

A. Isothermal experiments

The Johnson–Mehl–Avrami analysis gives the fraction of material transformed in an isothermal nucleation-and-growth process as[1,3]

$$x = 1 - \exp(-Kt^p), \tag{31}$$

where K incorporates the rates of nucleation and growth, and p, depending on the nucleation mechanism and the growth morphology, varies between 0.5 and 4.[1] The rate of enthalpy decrease in such a process is

$$\Delta H\frac{dx}{dt} = \Delta H\,pKt^{p-1}\exp(-Kt^p) = \Delta H p K^{1/p}[-\ln(1-x)]^{(p-1)/p}(1-x), \tag{32}$$

where ΔH is the total enthalpy difference between the transformed and untransformed state. Figure 1 shows the exothermic isothermal signals for a range of values of p. The common transformations have $p>1$, and their signal shows a *peak* at a nonzero time $t = [(p-1)/nK]^{1/n}$. Physically, the initial rise of the signal is the result of the increasing amount of material transformed as the growth front moves away from the nucleation sites. The eventual decrease occurs after impingement of the transformed regions.

A few unusual transformations, all occurring by one- or two-dimensional growth from a fixed number of specially distributed pre-existing nuclei, can have $p\leqslant 1$ and give a monotonically decreasing signal. These transformations have specific morphologies that can easily be identified by

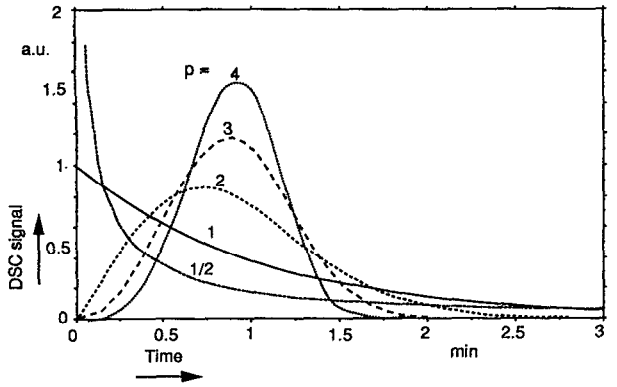

FIG. 1. Isothermal calorimetry signals for nucleation-and-growth processes described by Eq. (32). $K = 1$, and p is varied between 4 and 1/2.

microscopic observation. For example, $p = 1$ can correspond to uniform growth at a constant velocity from randomly oriented planes such as grain boundaries, to diffusion-controlled growth of widely spaced needles or plates, or to the diffusion-controlled thickening of long cylinders. Diffusion-controlled thickening of very large plates gives $p = 1/2$. An interesting, geometrically well-defined case is the one-dimensional growth of new phases in artificial multilayers, which also gives a monotonically decreasing signal if it is diffusion controlled.[18,19]

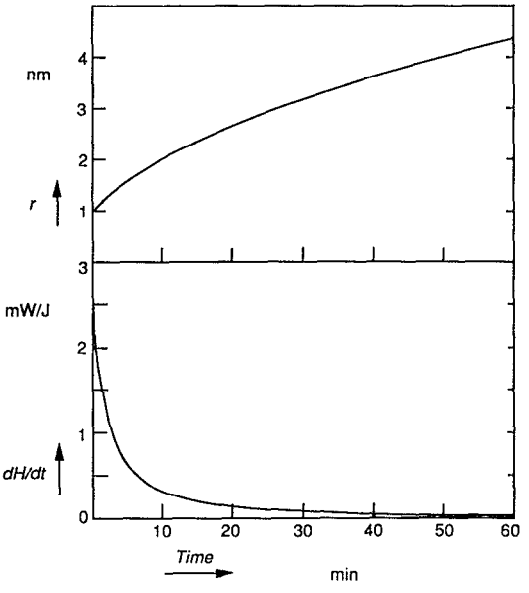

FIG. 2. Top: Isothermal evolution of the average grain radius [Eq. (8)]. Bottom: Corresponding enthalpy release rate [Eq. (13)]. The parameters are: $n = 2$, $r_0 = 10$ Å, $k(T) = 0.5$ Å^2/s. The units of dH/dt are normalized with respect to the total enthalpy H_0.

In isothermal normal grain growth, the calorimetric signal is given by Eq. (13). As shown in Fig. 2, this signal is *always monotonically decreasing*. Abnormal (or secondary) grain growth, on the other hand, in which a few grains grow at the expense of the others, produces a peak in the signal, since the amount of grain boundary area that is eliminated increases during the initial growth of the secondary grains, and decreases when the secondary grains impinge. The formalism for abnormal grain growth is discussed in more detail in Appendix B.

The qualitative difference between the isothermal signals for grain growth and for nucleation-and-growth can be used as a criterion for deciding if materials exhibiting broad diffraction halos have a truly amorphous (i.e., nonperiodic, liquidlike) structure, or are microcrystalline. If upon crystallization (i.e., transformation to a phase with sharp diffraction rings) a monotonically decreasing isothermal signal is observed, the transformation is one of grain growth, and the material is microcrystalline. Crystallization of a truly amorphous, liquidlike phase must occur by nucleation-and-growth of a new, crystalline phase, and the corresponding calorimetric signal should therefore show a peak. Most of the unusual conditions that can give monotonically decreasing signals in nucleation and growth cannot be found in a homogeneous amorphous phase (it does not contain grain boundaries, for example), and the remaining ones can easily be identified by microscopic observation of the morphology of the crystallization products. Obviously, one needs a structural probe in addition to calorimetry to ascertain that the exothermal signal analyzed indeed corresponds to crystallization.

B. Scanning experiments

In the analysis of phase transformations by nonisothermal calorimetry it is convenient to assume that the transformation rate depends only on state variables, such as the temperature and the fraction transformed at that instant, but not on the prior thermal history.[20] Henderson has published a critical paper on the validity of the application of the isothermal JMA equation [Eq. (31)] under nonisothermal conditions.[3] One type of experiment in which these conditions often apply is the crystallization of metallic glasses. Greer,[21] for example, has modeled the nucleation and growth of crystals in glassy $Fe_{80}B_{20}$ during linear heating by using the JMA equation in a series of short isothermal anneals. The curve corresponding to $p = 3$ in Fig. 3 is one of his results. A number of curves generated in a similar way for different values of p are shown as well. All peaks are asymmetrical, with a slower rise on the low-temperature side.

In normal grain growth, the enthalpy release rate in a scanning experiment is given by Eq. (14). Figure 4 shows the results for different variations in the initial grain size r_0, the activation enthalpy Q, and the prefactor of the rate constant, k_0. A comparison of these curves with the analogous ones for nucleation-and-growth (Fig. 5) reveals some interesting differences and similarities:

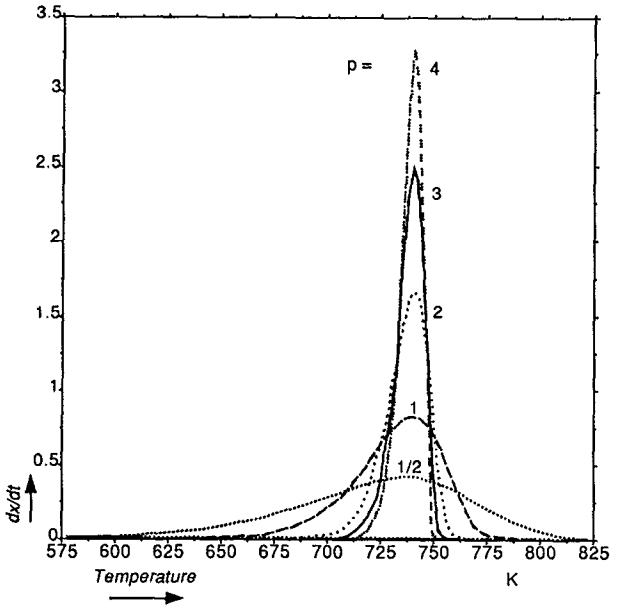

FIG. 3. Scanning calorimetry signal, at a heating rate of 40 K/min, from a nucleation-and-growth process, simulated by applying Eq. (32) to a series of short isothermal anneals. $K = K_0 \exp(-pQ/k_B T)$, $Q = 2.5$ eV, $K_0 = (2.1 \times 10^{17}\ \text{min}^{-1})^p$, and p is varied between 4 and 1/2. These values are chosen so that $p = 3$ corresponds to Greer's fit to the crystallization kinetics of $Fe_{80}B_{20}$.[21]

(i) The leading edge of the grain growth peak is steeper than the trailing edge. For the nucleation-and-growth peak it is the other way around.

(ii) Preannealing of a grain growth sample increases the initial grain size, r_0, which shifts the onset of the peak to *higher* temperatures and leads to a *narrower* transformation range [Fig. 4(a)]. Preannealing of a nucleation-and-growth sample increases the initially transformed fraction, which shifts the peak to *lower* temperatures and *broadens* it [Figure 5(a)].

(iii) An increase in the atomic jump frequency [through k_0 in Eq. (6) for grain growth, and the prefactor for K in Eq. (31)] has a qualitatively and quantitatively similar effect on both peaks: they shift to lower temperatures and become slightly more narrow [Figs. 4(b) and 5(b)].

(iv) A decrease in the activation enthalphy for atomic motion, with an adjustment in the prefactor to keep the peak at the same temperature, broadens the peaks to a similar degree in both cases [Figs. 4(c) and 5(c)].

In practice, it is not always straightforward to evaluate the shape of the scanning peaks. For example, the low-temperature part of a bulk crystallization peak may be influenced by surface crystallization,[22] the high-temperature part by the onset of a subsequent transformation to a different crystal structure (see example below), or the entire shape by a temperature dependence of a parameter assumed constant in the analysis. The shape of a scanning peak therefore gives at best an indication as to the nature of the transformation. Generally, one can say that for grain grain growth the peak is wider,[23] and that the total heat given off is considerably smaller than in a true crystallization (25% in the case discussed below, for example). The unambiguous determination of the transformation type must therefore come from isothermal experiments.

VIII. CASE STUDY: GRAIN GROWTH IN MICROQUASICRYSTALLINE Al-Mn FILMS.

$Al_{83}Mn_{17}$ films 5–7 μm thick were prepared by rf-sputtering in 0.3 Pa Ar pressure onto copper substrates at 60 °C. A Perkin-Elmer DSC-2 calorimeter was used for the study. The films were mechanically removed from the substrates as small flakes, which were stacked and sealed in standard aluminum calorimeter pans. The sample weights were between 1 and 1.5 mg.

Figure 6 shows scanning calorimetry traces taken at three different heating rates. Two transformations are observed. X-ray and electron microscope observations[8] show that the as-deposited material has broad, amorphouslike diffraction peaks. During the first transformation the diffraction pattern sharpens up continuously to a sharp, icosahedral one, and after the first scanning peak the microstructure consists of small (50 Å), equiaxed icosahedral grains. After the second scanning peak, the microstructure consists of somewhat larger, equiaxed periodic crystals. The transformation enthalpies are, in order, $\Delta H_1 = 250$ cal/mole and $\Delta H_2 = 910$ cal/mole.

The size and shape of the first scanning peak, shown in more detail in Fig. 7, already indicate that the first transformation is not standard crystallization by nucleation and growth: the peak is asymmetric with a steeper rising edge (the last part of the tail is obscured by the onset of the second transformation), and the transformation enthalpy is unusually small (only 25% of the typical heat of crystallization for an amorphous metal[24]).

Figure 8 shows a Kissinger plot [Eq. (23)] of the peak temperatures for the first transformation of Fig. 6. The slope of the straight line fit through the points gives $Q_1' = 2.52$ eV. A plot according to Eq. (22), which uses the correct frequency factor, gives $Q_1 = 2.59$ eV, indistinguishibly close to the Kissinger value.

In the isothermal experiments, the samples were heated up at 20 K/min to a temperature at the start of the first peak (563, 573, and 583 K), and held until the signal was no longer measurable. After cooling to room temperature, the sample was run again under identical conditions to establish the baseline, which was always perfectly horizontal and matched the zero of the signal. That the signals of Fig. 9 all decay monotonically, as derived above and shown in Fig. 2, demonstrates unambiguously that the transformation process is one of grain growth. The as-deposited material is therefore microquasicrystalline, consistent with its diffraction pattern being a broadened quasicrystalline powder pattern[8,17] and with the microstructure of rapidly quenched Al-Mn droplets.[4]

The total enthalpy released in the isothermal experiments, $H_0(T)$, is 222, 204, and 185 cal/

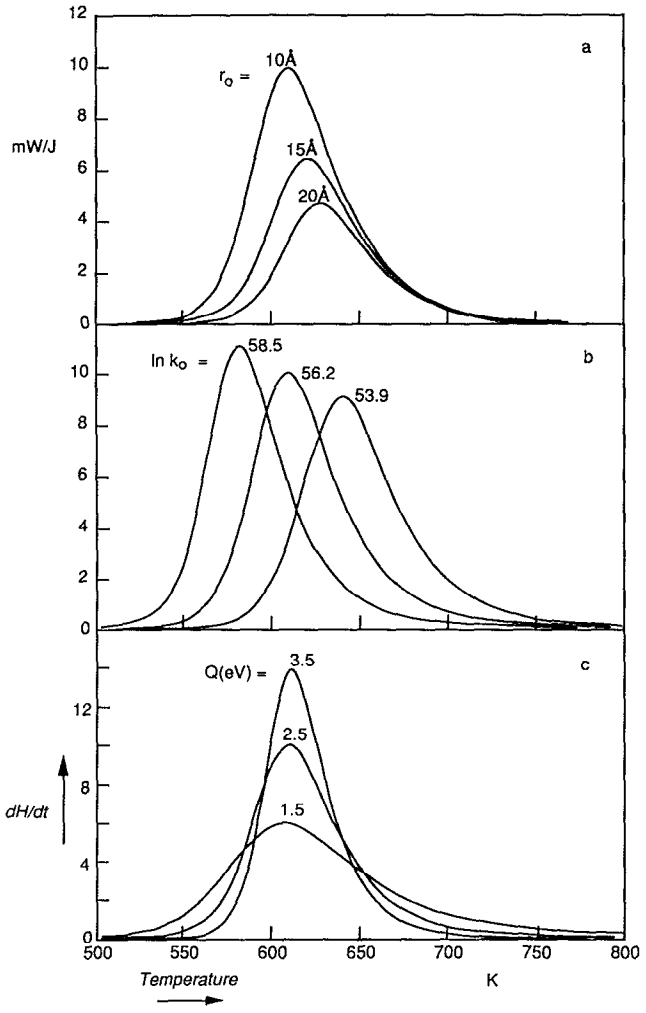

FIG. 4. Scanning calorimetry signal, at a heating rate of 40 K/min, from a grain growth process [Eq. (14)], showing the effect of changes in various parameters. Unless otherwise indicated the parameters are: $n = 2$, $r_0 = 10$ Å, $k_0 = 13 \times 10^{23}$ Å^2 K/s, $Q = 2.5$ eV. (a) Effect of preannealing (increasing the initial grain radius): $r_0 = 10$, 15, and 20 Å. (b) Effect of the atomic jump frequency: ln $k_0 = 58.5$, 56.2, 53.9 (Å^2 K/s). (c) Effect of the activation enthalpy, with k_0 adjusted to keep the peak temperature at 608 K: $Q = 1.5$, 2.5, 3.5 eV. ln $k_0 = 36.7$, 56.2, 75.4 (Å^2 K/s), respectively.

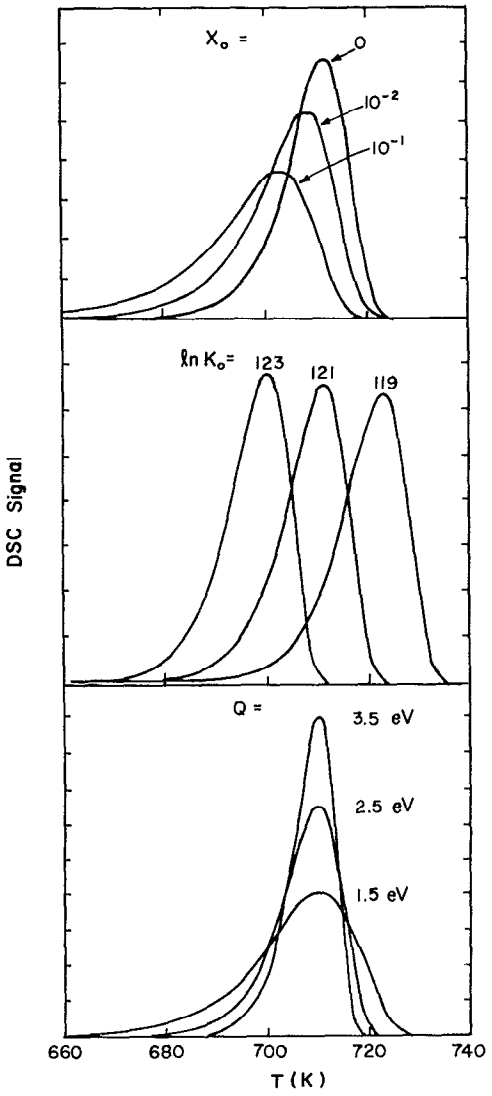

FIG. 5. Effect of the various parameters on the scanning calorimetry signal, at 10 K/min, for a nucleation-and-growth process. In all cases $p = 3$, and $Q = 2.5$ eV unless otherwise indicated. (a) Effect of preannealing (increasing the initial transformed fraction): $x_0 = 0$, 0.01, 0.1 [ln $K_0 = 121$ (min^{-3})]. (b) Effect of the atomic jump frequency: ln $K_0 = 119$, 121, 123 (min^{-3}). (c) Effect of the activation enthalpy, with K_0 adjusted to keep the maximum of the peak at 710 K: $Q = 1.5$, 2.5, 3.5 eV, ln $K_0 = 70.54$, 121, 171 (min^{-3}), respectively. After Greer.[21]

mole, respectively. The difference between these values and $\Delta H_1 = 250$ cal/mole measured in the scanning experiment is due to grain growth during heatup. Figure 10 shows a plot of the isothermal data according to Eq. (28), using $\tau = 3$, 2.24, and 0.65 min, respectively. The corresponding grain growth exponents, n, are 1.9 ± 0.2, close to the value $n = 2$ used in most theoretical models.

The activation enthalpy for the grain growth process can be determined by the procedure described in Sec. V. Figure 11 shows a plot of $\ln\{t_{1/2} H_0^n(T)/T\}$ vs $1/T$ for the three isothermals. The slope of the straight-line fit corresponds to $Q_1 = 2.2$ eV, which is similar to the value deter-

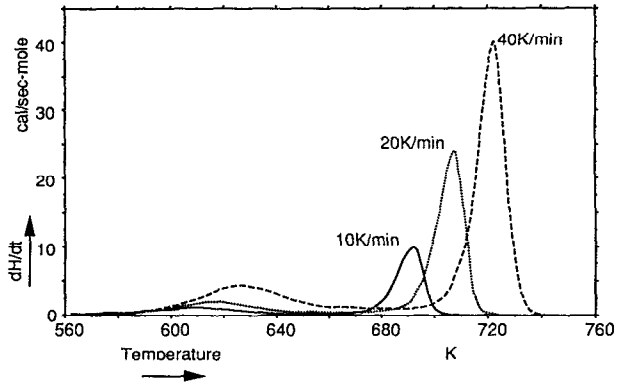

FIG. 6. Scanning calorimetry traces, at 10, 20, and 40 K/min, from $Al_{83}Mn_{17}$ sputtered thin films.

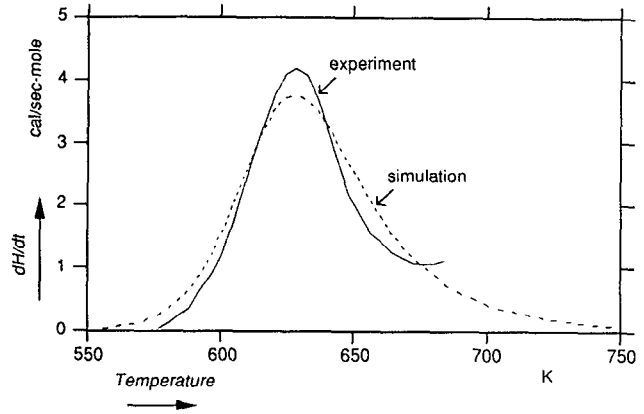

FIG. 7. Enlarged view of the first peak in Fig. 6 (40 K/min). The dashed line is a simulation using Eq. (14) and the parameters $r_0 = 16$ Å, $Q' = 2.52$ eV, $k_0' = 3\times10^{21}$ Å$^{1.9}$ s^{-1}, and $g\gamma = 0.273$ N/m.

mined for the process by the Kissinger method, which, as shown in Sec. III, can also be applied to a grain growth process.

The grain radius in the as-deposited material, r_0, was determined from the broadening of the diffraction peaks to be 16 Å, consistent with high-resolution electron microscopy observations.[8] If this is taken as the initial grain radius at the lowest isothermal testing temperature (563 K), Eq. (24) gives the kinetic coefficient: $k(563\text{ K}) = r_0^n/\tau(563\text{ K}) = 1.078$ Å$^{1.9}$ s^{-1}. Since the activation enthalpy, Q', is known from the Kissinger plot, the prefactor of the kinetic coefficient can be determined from Eq. (7): $k_0' = 4.316\times10^{22}$ Å$^{1.9}$ s^{-1}. The initial grain size of the higher-temperature isothermals can be calculated based on Eq. (10): $r_{0,T1}/r_{0,T2} = H_{0,T2}/H_{0,T1}$. Using these values, the isothermal runs can be simulated with Eq. (13). Figure 9

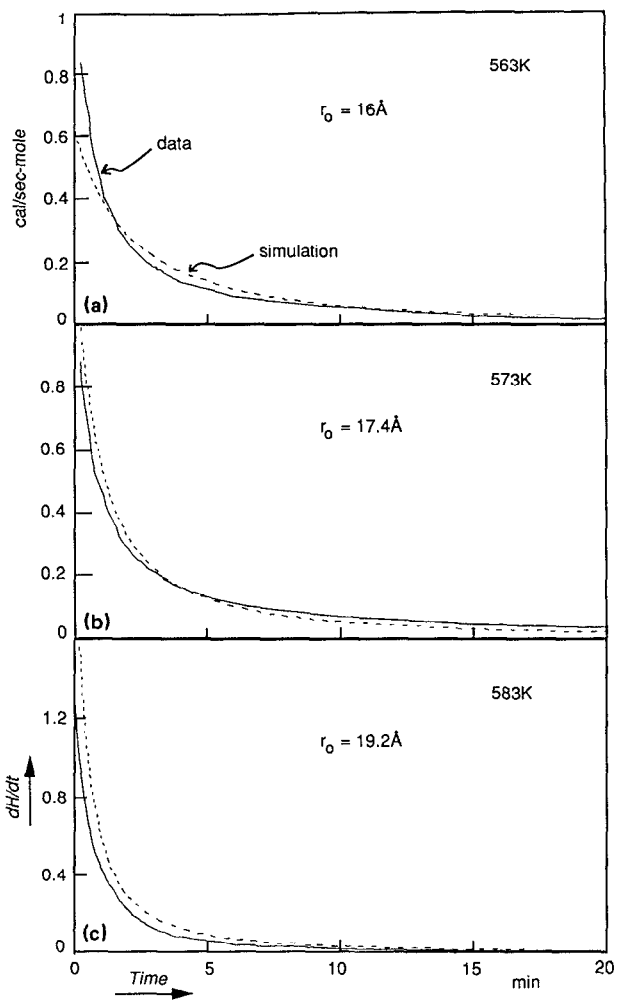

FIG. 9. Isothermal calorimetry traces at three temperatures from $Al_{83}Mn_{17}$ sputtered thin films. The dashed lines are simulations according to Eq. (13). Parameters: $Q' = 2.52$ eV, $k_0' = 4.316\times10^{22}$ Å$^{1.9}$ s^{-1}, $n = 1.9$, and (a) at 563 K: $r_0 = 16$ Å, $H_0 = 222$ cal/mole; (b) at 573 K: $r_0 = 17.4$ Å, $H_0 = 204$ cal/mole; (c) at 583 K: $r_0 = 19.2$ Å, $H_0 = 185$ cal/mole.

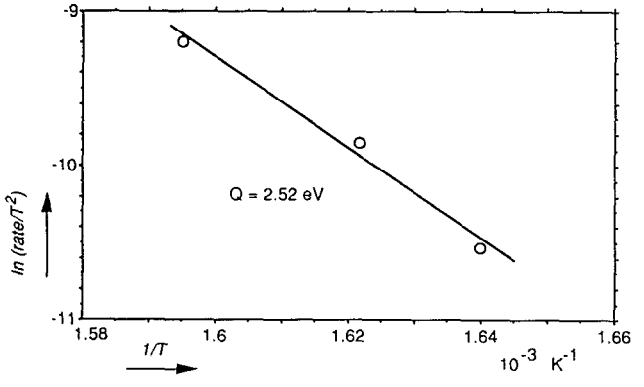

FIG. 8. Kissinger plot of the shift in the peak temperatures of the first transformation in Fig. 6 with heating rate.

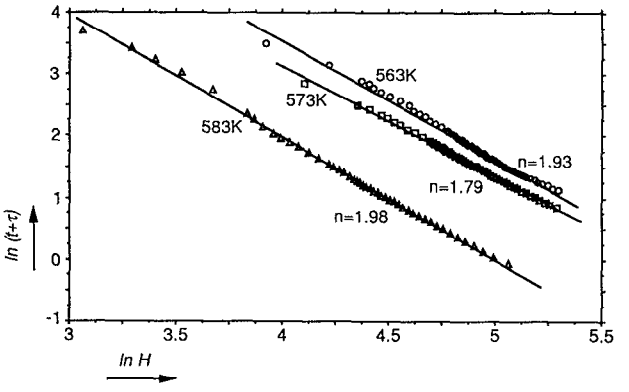

FIG. 10. Plot of the isothermal data according to Eq. (28), to determine the grain growth exponent. $n = 1.9 \pm 0.2$.

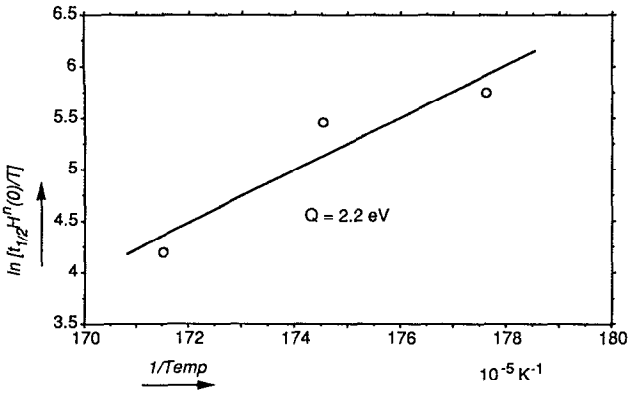

FIG. 11. Plot of the isothermal decay time according to Eq. (30) to determine the activation enthalpy. $Q = 2.2$ eV.

shows the comparison with the data. That the discrepancy between data and simulation is greatest in the initial growth stage is to be expected, since deviations from the macroscopic grain growth model are most likely to occur in this regime. For example, the contribution of the triple junctions to the average interfacial tension could be more substantial for the smallest grains.

The scanning runs can be simulated using Eq. (14). The dashed line in Fig. 7 shows the best fit to the data. That the parameters are not precisely the same in the three isothermal simulations and in the scanning simulation is most likely due to some temperature dependence of some of the parameters assumed to be constant in the theory, such as the interfacial tension.

The average enthalpic part of the interfacial tension, γ_H, is determined from the total transformation heat, $\Delta H_1 = 250$ cal/mole, measured in the scanning experiment and Eq. (10). Using a geometrical factor $g = 1.3 \pm 0.2$, as discussed in Sec. VI and Appendix A, and $V = 9.184$ cm^3/mole,[25] gives $\gamma_H = 0.14 \pm 0.03$ N/m. This value is about half of the average grain boundary energy in pure aluminum.[26]

ACKNOWLEDGMENTS

We thank K. G. Kreider for providing the films used in the case study, and S. C. Moss, J. L. Robertson, and K. Hiraga for useful discussions. This work has been supported by the National Science Foundation through the Harvard Materials Research Laboratory under contract No. DMR-86-14003 and by the Office of Naval Research under Contract No. N00014-85-K-0023. L.C.C. has been supported by a predoctoral fellowship from the IBM Corporation.

APPENDIX A: DETERMINATION OF THE GEOMETRICAL FACTOR g IN EQ. (10) FOR THE TOTAL INTERFACIAL ENTHALPY.

For a grain size distribution $P(r)$, the geometrical factor can be expressed as

$$g = \frac{\bar{r}(H/\gamma_H)}{V} = \frac{\bar{r}\, g_A \int 2\pi r^2 P(r)dr}{g_V \int \frac{4\pi}{3} r^3 P(r)dr} = \left(\frac{g_A}{g_V}\ \frac{3}{2}\right) \frac{\bar{r}\,\overline{r^2}}{\overline{r^3}}, \tag{A1}$$

where $\bar{r}$ is the mean grain radius, determined by either fitting the X-ray peak width or from TEM microstructure observations, H/γ_H is the total interfacial area, which can be calculated, assuming that all the grains have identical shape. The geometric factors g_A and g_V are introduced for, respectively, the area and volume correction arising from the spherical grain shape approximation. For cubic or tetrakaidekahedral (i.e., the Voronoi cell of the *b.c.c.* lattice[27]) grains the factor $(g_A/g_V\ 3/2)$ is, respectively, 1.86 or 1.65. Depending on the nature of $P(r)$, the size distribution factor, $(\overline{rr^2}/\overline{r^3})$, varies. For identical grains, $P(r) = \delta(r - \bar{r})$, this factor is 1. For a log-normal distribution function,[28]

$$P(r) = \frac{b}{\sqrt{\pi} r_m} \exp\left(\frac{-1}{4b^2}\right) \exp\left\{-b^2\left[\ln\left(\frac{r}{r_m}\right)\right]^2\right\}, \tag{A2}$$

where r_m is the most probable grain radius, and b is a constant, $(\overline{rr^2}/\overline{r^3}) = \exp(-1/b^2)$. This factor approaches 1 for a sharply peaked distribution (i.e. for large b). Experiments[29,30] and computer simulations[31,32] give $b \sim 2$–2.5, corresponding to $(\overline{rr^2}/\overline{r^3})$ between 0.778–0.852. For the Wagner-Hillert[11,12] distribution

$$P(r) = (2e)^3 \frac{3u}{(2-u)^5} \exp\left(\frac{-6}{2-u}\right), \tag{A3}$$

where $u = r/r_{cr}$, and r_{cr} is a critical radius such that grains with $r > r_{cr}$ grow, and those with $r < r_{cr}$ shrink, the size distribution factor becomes 0.826.
For the Louat distribution[33]

$$P(r) = \left(\frac{2a^2}{r_m^2}\right) r \exp\left[-a^2\left(\frac{r}{r_m}\right)^2\right], \tag{A4}$$

where r_m is the most probable grain radius, and a is a constant, $(\overline{rr^2}/\overline{r^3}) = 2/3$, independent of a.

Considering all these factors, we estimate the grain size and shape distribution factor g in Eq. (10) to be 1.3 ± 0.2.

APPENDIX B: ABNORMAL GRAIN GROWTH

In normal grain growth the size of the grains at one time remains relatively uniform. In abnormal grain growth, a few grains grow more rapidly than the average grains and the difference in the sizes increases. It has been shown that, if uniform grain boundary energy is the only factor affecting boundary motion and the mobility is independent of grain size, an abnormally large grain in a matrix of normal grains does not grow at a higher relative rate than its neighbors.[13] Therefore, if abnormal grain growth is observed, it must be the result of factors such as anisotropic surface energy or the

grain size dependence of mobility and/or surface energy, so that a grain that is substantially larger than average grows at a higher absolute rate than the surrounding normal grains. The following analysis shows that the rate of enthalpy release in an abnormal grain growth process mimics that of the nucleation-and-growth process.

Let r_1 and r_2 be, respectively, the average normal and abnormal grain radii in a bimodal grain size distribution, with $r_2 \gg r_1$, and $\dot{r}_2(t) \gg \dot{r}_1(t)$. Under these conditions, r_1 can be considered as a time-independent constant. As illustrated in Fig. 12, the abnormal grain grows at the expense of surrounding normal grains, and the enthalpy release (per abnormal grain) associated with this is

$$\Delta H = g' \left(\frac{4\pi r_2^2 \Delta r_2}{\frac{4}{3}\pi r_1^3} \right) 2\pi r_1^2 \gamma_H = \frac{g\gamma_H}{r_1} (4\pi r_2^2 \Delta r_2), \tag{B1}$$

where $4\pi r_2^2 \Delta r_2$ is the volume increase per abnormal grain if there is no impingement between nearby abnormal grains. If x is the volume fraction of abnormal grains, taking into account the impingement effect, and V is the total volume of the material, $(\dot{x}V)$ represents the rate of the volume transferred from normal to abnormal grains. Eq. (B 1) can be rewritten as

$$\dot{H} = \frac{g\gamma_H V}{r_1} \dot{x}. \tag{B2}$$

The volume fraction, x, transformed from normal to abnormal grains is related to the extended volume fraction (if there were no overlap), x_{ex}, by the Avrami equation:

$$x = 1 - \exp(-x_{ex}). \tag{B3}$$

If the number of abnormal grains remains the same, the time dependence of the extended volume fraction can be expressed as

$$x_{ex}(t) = \left(\frac{V_2(0)}{(4\pi/3) r_2^3(0)} \right) \frac{(4\pi/3) r_2^3(t)}{V} = x_0 \left(\frac{r_2(t)}{r_2(0)} \right)^3, \tag{B4}$$

where $V_2(0)$ and $x_0 = V_2(0)/V$ are, respectively, the initial volume and the initial volume fraction of abnormal grains.

Since the driving force for abnormal grain growth is the curvature of the neighboring normal grains, which changes negligibly with time, the abnormal grain radius usually increases linearly with time:[10,12]

$$r_2(t) = r_2(0) + k(T)t. \tag{B5}$$

Combining Eqs. (B3)–(B5) gives the volume fraction transformed isothermally:

$$x = 1 - \exp[-x_0(1 + ft)^3], \tag{B6}$$

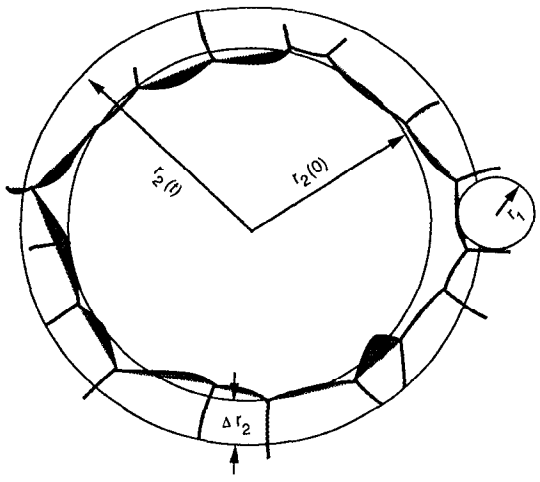

FIG. 12. Schematic diagram of the growth of an abnormal grain.

where $f = k/r_2(0)$, is a frequency factor. Although Eq. (B6) is more complicated than the JMA form of Eq. (31), under the usual condition $ft \gg 1$, it mimics the JMA equation with exponent 3. The isothermal signal then shows a peak at nonzero time.

Not only are the qualitative shapes of the isothermal signals for abnormal grain growth and for nucleation-and-growth indistinguishable, the morphology resulting from both processes is also very similar. The only remaining calorimetric indication of a grain growth process in this case is the size of the total enthalpy released, which, as mentioned above, is noticeably smaller for a coarsening process than for nucleation-and-growth of crystals in a liquidlike phase.

[1] J. W. Christian, *The Theory of Transformations in Metals and Alloys*, 2nd ed. (Pergamon, Oxford, 1975).
[2] H. E. Kissinger, Anal. Chem. **29**, 1702 (1957).
[3] D. W. Henderson, J. Non-Cryst. Solids **30**, 301 (1979).
[4] L. A. Bendersky and S. D. Ridder, J. Mat. Res. **1**, 415 (1986).
[5] C. N. J. Wagner, T. B. Light, N. C. Halder, and W. E. Lukens, J. Appl. Phys. **39**, 3690 (1968).
[6] R. W. Siegel, S. Ramaswamy, H. Hahn, Li Zongquan, Lu Ting, and R. Gronsky, J Mat. Res. **3**, 1367 (1988).
[7] L. C. Chen and F. Spaepen, Nature **336**, 336 (1988).
[8] L. C. Chen, F. Spaepen, J. L. Robertson, S. C. Moss, and K. Hiraga, (unpublished).
[9] H. V. Atkinson, Acta Metall. **36**, 469 (1988).
[10] J. E. Burke and D. Turnbull, Prog. Metal Phys. **3**, 220 (1952).
[11] C. Wagner, Z. Elektrochem. **65**, 581 (1961).
[12] M. Hillert, Acta Metall. **13**, 227 (1965).
[13] C. V. Thompson, H. J. Frost, and F. Spaepen, Acta Metall. **35**, 887 (1987).
[14] H. Eyring, J. Chem. Phys. **3**, 107 (1935).
[15] C. A. Wert, Phys. Rev. **79**, 601 (1950).
[16] M. Abramowitz and I. E. Stegun, *Handbook of Mathematical Functions* (Dover, New York, 1968), p.231.
[17] J. L. Robertson, S. C. Moss, and K. G. Kreider, Phys. Rev. Lett. **60**, 2062 (1988).
[18] F. Spaepen and C. V. Thompson, Appl. Surf. Sci. **38**, 1 (1989).
[19] L. A. Clevenger and C. V. Thompson, J. Appl. Phys. **67**, 1325 (1990).
[20] M. Avrami, J. Chem. Phys. **7**, 1103 (1939); **8**, 212 (1940); **9**, 177 (1941).
[21] A. L. Greer, Acta Metall. **30**, 171 (1982).

[22] K. F. Kelton and F. Spaepen, Acta Metall. **33**, 455 (1985).
[23] J. C. Malaurent, J. Dixmier, and C. Mazier, C. R. Acad. Sci. Paris **275 B**, 743 (1972).
[24] L. Battezzati and E. Garrone, Z. Metallk. **75**, 305 (1984).
[25] D. Turnbull, Acta Metall. **38**, 243 (1990).
[26] H. Gleiter and B. Chalmers, Prog. Mat. Sci. **16**, 13 (1972).
[27] C. S. Smith, in *Metal Interfaces* (ASM, Cleveland, 1952), p. 65.
[28] P. Feltham, Acta Metall. **5**, 97 (1957).
[29] S. F. Kurtz and F. M. A. Carpay, J. Appl. Phys. **51**, 5725 (1980).
[30] J. E. Palmer, C. V. Thompson, and H. I. Smith, J. Appl. Phys. **62**, 2492 (1987).
[31] H. J. Frost, C. V. Thompson, and C. T. Walton, Acta Metall., **38**, 1455 (1990).
[32] D. J. Srolovitz, M. P. Anderson, P. S. Sahni, and G. S. Grest, Acta Metall. **32**, 793 (1984).
[33] N. P. Louat, Acta Metall. **22**, 721 (1974).